# Three-dimensional nature of normal and superconducting states in $BaNi_2P_2$ single crystals with the $ThCr_2Si_2$-type structure

Y. Tomioka,[1,2] S. Ishida,[1,2,3] M. Nakajima,[1,2,3] T. Ito,[1,2] H. Kito,[1,2] A. Iyo,[1,2] H. Eisaki,[1,2] and S. Uchida[3]
[1]*Nano Electronics Research Institute (NeRI), National Institute of Advanced Industrial Science and Technology (AIST), Tsukuba 305-8562, Japan*
[2]*JST, Transformative Research-Project on Iron Pnictides (TRIP), 5 Sanbancho, chiyoda-ku, Tokyo 102-0075, Japan*
[3]*Department of Physics, University of Tokyo, 7-3-1 Hongo Bunkyo-ku, Tokyo 113-8656, Japan*
(Received 2 March 2009; published 29 April 2009)

Normal and superconducting states of $BaNi_2P_2$ single crystals ($T_C \sim 2.4$ K) have been studied. Anisotropy of resistivity is comparable with that of upper critical fields, indicating the effective mass estimated in the normal state is nearly the same as that in the superconducting state. From magnetization hysteresis with a weak vortex pinning, lower critical fields are estimated. Hall effect is explained by a two-carrier model consistent with a multiple-band with both hole and electron characters. It has been proved that $BaNi_2P_2$ is an anisotropic three-dimensional intermetallic superconductor.

DOI: 10.1103/PhysRevB.79.132506 PACS number(s): 74.70.Dd, 74.25.Dw, 74.25.Fy, 74.25.Ha

Recently, a new class of high-temperature superconductivity has been discovered in the iron-arsenide layered compounds with the ZrCuSiAs structure, i.e., oxypnictides, $LaFeAs(O_{1-x}F_x)$,[1,2] and those with the $ThCr_2Si_2$ structure, $Ba_{1-x}K_xFe_2As_2$.[3] In the fluorine-free and oxygen-deficient compound, $NdFeAsO_{1-y}$ ($0.3 \leq y \leq 0.8$), the critical temperature, $T_C$ becomes as high as 53 K.[4] Besides these iron-arsenide compounds, pioneering superconductors have earlier been found, although the critical temperatures are lower.[5–8] As described in Ref. 8, a superconducting transition occurs in the nickel-based phosphide, $BaNi_2P_2$ ($T_C \sim 3$ K), the crystal structure of which is the same as $BaFe_2As_2$, the parent compound for high-temperature superconductivity. Similarly to cuprates, the newly discovered iron- or nickel-based superconductors have two-dimensional crystal structures, and the carrier is doped from the adjacent layers. Calculated band structures of LaOFeAs and LaOFeP,[9] on the other hand, indicate that the Fermi level is crossed by five bands with mainly Fe character, which is different from a single band feature in cuprates. For $BaFe_2As_2$, as described in Ref. 10, the Fermi surface is similar to that of LaOFeAs.

In this Brief Report, we report the normal and superconducting states of $BaNi_2P_2$ single crystals prepared by the high-pressure synthesis method using the cubic-anvil-type apparatus (Riken CAP-07).[4] The dimensions of the crystals used for the in-plane and out-of-plane resistivity measurements are about $0.50 \times 0.13 \times 0.013$ mm$^3$ and $0.63 \times 0.56 \times 0.025$ mm$^3$, respectively, with the shortest edge parallel to the $c$ axis. For the out-of-plane resistivity, the current electrodes on both surfaces of the crystal are drawn in a shape of annular ring with use of gold paste. The voltage electrodes are at the center of the ring.[11] Resistivity in magnetic fields has been measured in a cryostat equipped with a superconducting magnet. For Hall-effect measurement, the gold wires are attached to a crystal through the electrodes made by gold paste, and the magnetic field is applied perpendicular to the plane with the current in plane. The zero-field-cooled (ZFC) and field-cooled (FC) magnetization has been measured by a superconducting quantum interference device (SQUID) magnetometer (MPMS, Quantum Design Inc.). After the crystal is cooled down to the lowest temperature (1.76 K) in zero field, the magnetic field is applied, and the ZFC magnetization is measured with increasing temperature. Subsequently, the FC magnetization is measured with decreasing temperature in a same magnetic field.

Figure 1 shows temperature profiles of the in-plane, $\rho_\parallel$, and out-of-plane, $\rho_\perp$, resistivities of the $BaNi_2P_2$ single crystals, respectively. The value of $\rho_\parallel$ ($\rho_\perp$) at 300 K is about 80(500) $\mu\Omega$ cm, and as shown in the inset, the residual resistivity is 4.15(14.4) $\mu\Omega$ cm, which leads to that the residual resistivity ratio $[\rho(300\ \mathrm{K})/\rho(3\ \mathrm{K})]$ is 18.7 (34.3) for in plane (out of plane). The anisotropy of resistivity, $\rho_\perp/\rho_\parallel$ is weakly dependent on temperature, and it is $\sim$6.3 at 300 K much smaller than that reported for the nondoped iron-arsenide compounds, $AFe_2As_2$ ($A$=Ba, Sr, and Ca).[12–14] For $T \leq 25$ K $\rho_\parallel$ is empirically fitted by $\rho = \rho_0 + AT^n$ with $\rho_0 = 4.15$ $\mu\Omega$ cm, $A = 7.78 \times 10^{-8}$ $\mu\Omega$ cm K$^{-n}$, and $n = 5$. As shown in this figure, temperature dependence of both in-plane and out-of-plane resistivities seems to cross over from linear at high temperatures to power law, $T^n$ at low temperatures. A detailed analysis will be published in Ref. 15. As

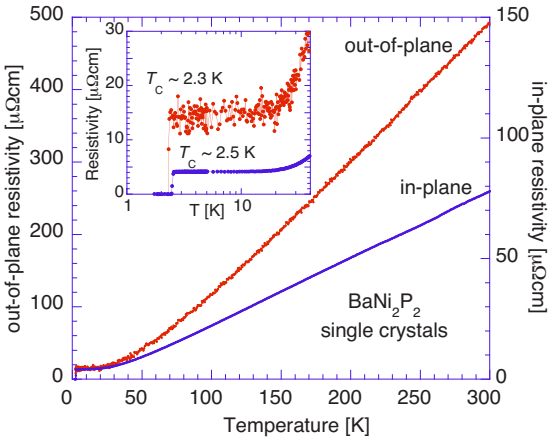


FIG. 1. (Color online) Temperature profiles of the in-plane, $\rho_\parallel$, and out-of-plane, $\rho_\perp$, resistivity for the $BaNi_2P_2$ single crystals, respectively. Inset shows the blow up below 40 K.

 

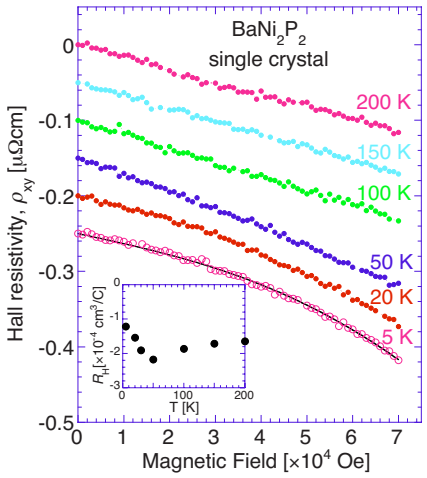


FIG. 2. (Color online) The magnetic field dependence of the Hall resistivity, $\rho_{xy}$ of a $BaNi_2P_2$ single crystal taken at several temperatures. The thick line for $\rho_{xy}$ at 5 K is the calculated result from Eq. (1) that $\rho_{xy}=-(1/e)H[n_e\mu_e^2-n_h\mu_h^2+(n_e-n_h)\mu_e^2\mu_h^2H^2]/[(n_e\mu_e+n_h\mu_h)^2+(n_e-n_h)^2\mu_e^2\mu_h^2H^2]$ with $n_e(n_h)=6.52\times10^{21}(3.90\times10^{20})$ cm$^{-3}$, and $\mu_e(\mu_h)=189(688)$ cm$^2$ V$^{-1}$ s$^{-1}$ ($n_h/n_e=0.060$ and $\mu_h/\mu_e=3.65$). Inset shows temperature variation in the Hall coefficient, $R_H$ determined from $d\rho_{xy}/dH$ at $H=0$.

temperature decreases, a superconducting state becomes prevailing. The critical temperature as a midpoint of the transition is 2.51 and 2.31 K for in plane and out of plane, respectively. Although from Fig. 1 the anisotropy ratio is weakly dependent on temperature, the scattering mechanism seems to be nearly common for both directions, and the anisotropy seems to originate from anisotropic mass ($\rho_\perp/\rho_\parallel\sim m_\perp^*/m_\parallel^*$). Figure 1 indicates that a rather usual electron-phonon scattering seems to be dominant for the resistivity of the $BaNi_2P_2$ single crystal.

Figure 2 shows the magnetic field dependence of Hall resistivity, $\rho_{xy}$ of a $BaNi_2P_2$ single crystal taken at several temperatures. In Fig. 2, nearly linear dependence of $\rho_{xy}$ on magnetic fields is seen at high temperatures, while nonlinear behavior is seen at low temperatures ($T<50$ K). Temperature variations in $R_H$ determined from $d\rho_{xy}/dH$ at $H=0$ are indicated in the inset. The $R_H$ estimated is negative in the magnitude of $10^{-4}$ cm$^3$/C, and the carrier numbers, $n$ is estimated to be in the magnitude of $10^{22}$ cm$^{-3}$ from a relation that $R_H=-1/(en)$, which is equivalent to 3–5 electrons per a formula unit of $BaNi_2P_2$.

TABLE I. Carrier numbers of two hole surfaces (band 25 and 26) and two electron surfaces (band 27 and 28) of $BaNi_2P_2$ (Ref. 16).

| | Carrier numbers per a formula unit of $BaNi_2P_2$ | Carrier numbers [/cm$^3$] |
|---|---|---|
| Band 25 (hole) | 0.06 | $6.52\times10^{20}$ |
| Band 26 (hole) | 0.88 | $9.56\times10^{21}$ |
| Band 27 (electron) | 0.6 | $6.52\times10^{21}$ |
| Band 28 (electron) | 0.34 | $3.69\times10^{21}$ |

A multiple Fermi surface with electron and hole characters could partly cancel out the Hall effect. As described in Ref. 16, two electron surfaces and two hole ones are found by de Haas–van Alphen (dHvA) oscillation, and their carrier numbers are listed in Table I. In a two-carrier model, Hall resistivity is expressed by an equation that[17]

$$\rho_{xy}=-(1/e)H[n_e\mu_e^2-n_h\mu_h^2+(n_e-n_h)\times\mu_e^2\mu_h^2H^2]/[(n_e\mu_e+n_h\mu_h)^2+(n_e-n_h)^2\mu_e^2\mu_h^2H^2] \quad (1)$$

where $n_e$ and $\mu_e$ ($n_h$ and $\mu_h$) are carrier numbers and mobility of electrons (holes), respectively. If we assume $n_e$ in Eq. (1) as that of band 27 in Ref. 16, we get $n_e=6.52\times10^{21}$ cm$^{-3}$, and $1/(n_ee)=-9.53\times10^{-4}$ cm$^3$/C. With use of the residual resistivity from Fig. 1 ($\rho_{\parallel0}=4.1$ $\mu\Omega$ cm), the dotted line for $\rho_{xy}$ at 5 K in Fig. 2 is the calculated result

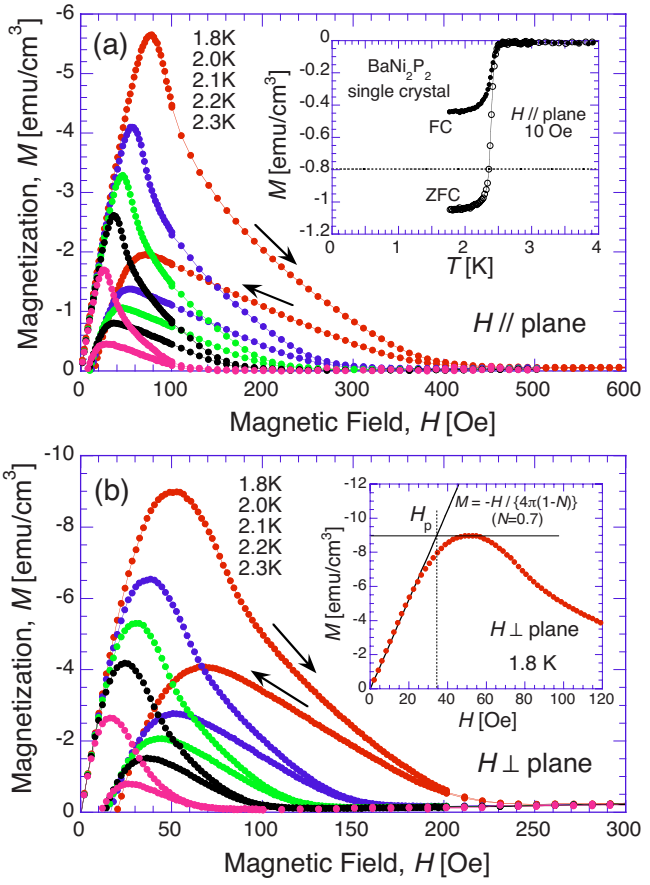


FIG. 3. (Color online) Temperature variations in the magnetization hysteresis of a $BaNi_2P_2$ single crystal for the magnetic field (a) parallel and (b) perpendicular to plane. The dimensions of the crystal are about $0.55\times0.26\times0.07$ mm$^3$ with the shortest edge parallel to the $c$ axis. The inset of (a) shows the zero-field-cooled and field-cooled magnetization taken at 10 Oe. A level of perfect diamagnetism is denoted as the dashed line. The inset of (b) indicates the estimation of the field, $H_p$ at which an extrapolation of perfect diamagnetism, $M=-H/\{4\pi(1-N)\}$ ($N$; demagnetizing factors) meets a level of the minimum magnetization (Ref. 19). The demagnetizing factors are 0.11 and 0.7 for the field parallel and perpendicular to the plane, respectively.

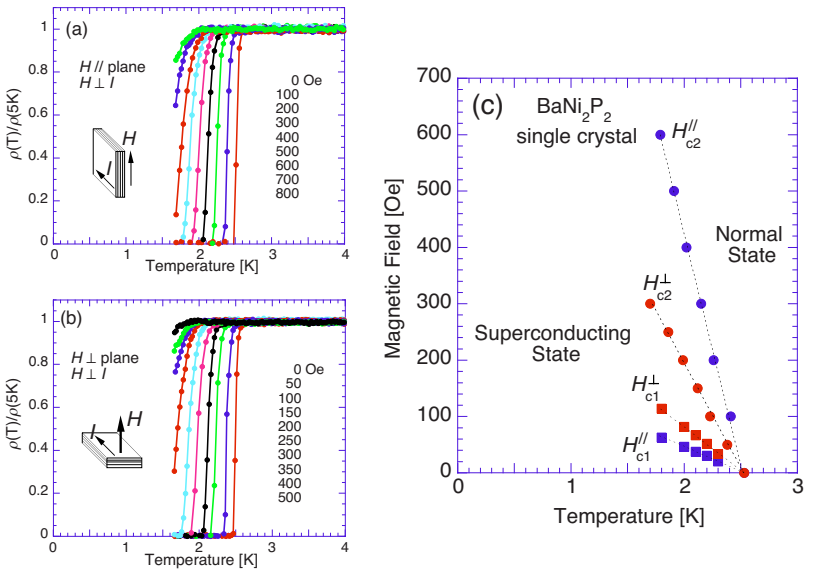


FIG. 4. (Color online) Temperature profiles of the in-plane resistivity normalized at 5 K for the magnetic field (a) parallel and (b) perpendicular to plane with the transport current perpendicular to field. (c) The lower (closed squares) and upper critical fields (closed circles) of $BaNi_2P_2$ single crystals for both magnetic field parallel and perpendicular to plane.

from Eq. (1) with $n_e(n_h)=6.52\times10^{21}(3.90\times10^{20})$ $cm^{-3}$, and $\mu_e$ $(\mu_h)=189(688)$ $cm^2\ V^{-1}\ s^{-1}$ $[n_h/n_e=0.060$ and $\mu_h/\mu_e=3.65]$, which are obtained by fitting $\rho_{xy}$ at 5 K. The estimated $n_h$ is comparable with that of band 25 in Ref. 16.

We have also measured the magnetoresistance (MR), $[\rho_\parallel(H)-\rho_\parallel(0)]/\rho_\parallel(0)$ at 5 K for magnetic field perpendicular to the plane ($H\perp$ plane) and the transport current in plane. It has been indicated that the MR is positive and almost linearly dependent on $H^2$, the magnitude of which is comparable with the value expected from the parameters obtained from the field-dependent Hall resistivity. The detail of the analysis is published in Ref. 15. Figure 2 thus indicates that transport properties of $BaNi_2P_2$ are composed of not only electrons but also holes with smaller carrier numbers and higher mobility, being consistent with the results described in Ref. 16.

In Fig. 3, are shown temperature variations of the magnetization hysteresis ($M$-$H$ curves) for magnetic field parallel ($H\parallel$ plane) (a) and perpendicular to the plane ($H\perp$ plane) (b), respectively. The inset of Fig. 3(a) indicates the ZFC and FC magnetization for $H\parallel$ plane taken at 10 Oe. In the inset, the magnitude of the ZFC magnetization at the lowest temperature exceeds perfect diamagnetism (dashed line) due to a demagnetizing effect,[18] and that of the FC magnetization reaches about 56%, the values of which are enough for bulk superconductivity.

As shown in the $M$-$H$ curves for both $H\parallel$ and $\perp$ plane, the discrepancies between the field-increasing and decreasing processes are not pronounced, indicating a rather weak vortex pinning. In the present study, the lower critical field, $H_{c1}$ is approximated from the penetration field, $H_p$ at which an extrapolation of perfect diamagnetism, $M=-H/\{4\pi(1-N)\}$ ($N$ being demagnetizing factors[18]) meets a level of the minimum magnetization,[19] as shown in the inset of Fig. 3(b), although it might overestimate lower critical field. The demagnetizing factor is 0.11 (0.7) for $H\parallel$ plane ($H\parallel$ plane), which is estimated from the initial magnetization vs $H$ at $H\ll H_p$. From a relation that $H_{c1}=H_p/(1-N)$,[19] the lower critical field is estimated at 52 (82) Oe for $H\parallel$ plane ($H\perp$ plane) at $T=2$ K, which are comparable with the results in the earlier work.[8]

Figure 4 shows temperature profiles of $\rho_\parallel$ normalized at 5 K for $H\parallel$ plane (a) and $\perp$ plane (b) of the same crystal used for the measurement of in-plane resistivity in Fig. 1. In Figs. 4(a) and 4(b), the transport current is perpendicular to field ($H\perp I$). In these figures, a broadening of the resistive transition with increase in field is not pronounced, and the transition temperature, $T_C(H)$ may be defined as the midpoint of the resistive transition. A state with finite resistivity at $T=1.6$ K for $H\parallel$ plane ($\perp$ plane) starts to be seen at $H\geq600$ (300) Oe. A rather usual resistive transition without broadening as shown in these figures is also seen in $Sr_{0.6}K_{0.4}Fe_2As_2$ with small anisotropy of resistivity[13] although both $T_C$ and critical fields of $Sr_{0.6}K_{0.4}Fe_2As_2$ are much higher than those of $BaNi_2P_2$.

In Fig. 4(c), with use of the field dependence of $T_C(H)$ as shown in Figs. 4(a) and 4(b), are indicated the upper critical field for $H\parallel$ plane, $H_{c2}^\parallel$ and that for $H\perp$ plane, $H_{c2}^\perp$. In Fig. 4(c), the lower critical fields for both directions are also indicated. From the relation that $H_{c2}(0)=0.69|dH_{c2}(T)/dT|_{T=TC}$ $T_C$,[20] $H_{c2}^\parallel(0)$ $(H_{c2}^\perp(0))$ is estimated about 1410 (650) Oe. From the equation that $H_{c2}^\perp(0)$ $(H_{c2}^\parallel(0))=\phi_0/(2\pi\xi_\parallel^2)$ $(\phi_0/(2\pi\xi_\parallel\xi_\perp))$, furthermore, the in-plane (out-of-plane) coherence length $\xi_\parallel$ $(\xi_\perp)$ is estimated about 710(330) Å. The ratio, $H_{c2}^\parallel(0)/H_{c2}^\perp(0)$ $(=(m_\perp^*/m_\parallel^*)^{1/2})$ is about 2.2, which is comparable with that of resistivity, $(\rho_\perp/\rho_\parallel)^{1/2}\sim2.5$. These results indicate that $BaNi_2P_2$ single crystal is a rather conventional type II superconductor with three-dimensional nature.

Band calculation of $BaNi_2P_2$ shows that multiple bands cross the Fermi level and dispersion exists both along in-plane and out-of-plane directions.[21] Although there is at present no publication on the Fermi surface of the compound, we may expect similar Fermi surface as that of $BaFe_2As_2$ (Ref. 10) that has more dispersion along the out-of-plane direction than that of LaOFeAs.[10] Therefore, three-dimensional nature of $BaNi_2P_2$ may be a natural consequence.

In summary, we have studied the normal and superconducting states of $BaNi_2P_2$ single crystals prepared by the

high-pressure synthesis method. Temperature dependence of resistivity is nearly the same both for the in-plane and out-of-plane directions, and the ratio of effective mass, $(m^*_\perp/m^*_\parallel)^{1/2}$ estimated from the anisotropy of resistivity is $\sim$2.5. The negative Hall coefficient in the magnitude of $10^{-4}$ $cm^3/C$ and the nonlinear field dependence of Hall resistivity at low temperatures are explained by a two-carrier model. *M-H* curves in the superconducting state show small hysteresis, characteristic for a weak vortex pinning, and the lower critical fields are estimated. From the resistive transition in magnetic fields, the upper critical field is estimated as $H^\parallel_{c2}(0)$ $(H^\perp_{c2}(0)) \sim 1410(650)$ Oe for *H* parallel (perpendicular) to the plane. The in-plane (out-of-plane) coherence length is $\xi_\parallel$ $(\xi_\perp) \sim 710(330)$ Å. The ratio of effective mass from the upper critical fields is about 2.2, which is comparable to that obtained in the normal state. It has been proved in present study that the $BaNi_2P_2$ compound is a three-dimensional anisotropic superconductor, which may be in contrast to superconductivity with higher $T_C$ of the hole-doped $AFe_2As_2$ ($A$=Ba, Sr, and Ca) with the same crystal structure.

We would like to acknowledge H. Aoki, K. Kuroki, S. Onari, and I. Hase for stimulus discussions.

[1] Y. Kamihara, T. Watanabe, M. Hirano and H. Hosono, J. Am. Chem. Soc. **130**, 3296 (2008).
[2] H. Takahashi, K. Igawa, K. Arii, Y. Kamihara, M. Hirano, and H. Hosono, Nature (London) **453**, 376 (2008).
[3] M. Rötter, M. Tegel, and D. Johrendt, Phys. Rev. Lett. **101**, 107006 (2008).
[4] H. Kito, H. Eisaki, and A. Iyo, J. Phys. Soc. Jpn. **77**, 063707 (2008).
[5] Y. Kamihara, H. Hiramatsu, M. Hirano, R. Kawamura, H. Yanagi, T. Kamiya, and H. Hosono, J. Am. Chem. Soc. **128**, 10012 (2006).
[6] T. Watanabe, H. Yanagi, T. Kamiya, Y. Kamihara, H. Hiramatsu, M. Hirano, and H. Hosono, Inorg. Chem. **46**, 7719 (2007).
[7] T. Watanabe, H. Yanagi, Y. Kamihara, T. Kamiya, M. Hirano, and H. Hosono, Inorg. Chem. **46**, 7719 (2007).
[8] T. Mine, H. Yanagi, T. Kamiya, Y. Kamihara, M. Hirano, and H. Hosono, Solid State Commun. **147**, 111 (2008).
[9] V. Vildosola, L. Pourovskii, R. Arita, S. Biermann, and A. Georges, Phys. Rev. B **78**, 064518 (2008).
[10] I. A. Nekrasov, Z. V. Pchelkina, and M. V. Sadovskii, JETP Lett. **88**, 144 (2008).
[11] T. Motohashi, Y. Nakayama, T. Fujita, K. Kitazawa, J. Shimoyama, and K. Kishio, Phys. Rev. B **59**, 14080 (1999).
[12] X. F. Wang, T. Wu, G. Wu, H. Chen, Y. L. Xie, J. J. Ying, Y. J. Yan, R. H. Liu, and X. H. Chen, Phys. Rev. Lett. **102**, 117005 (2009).
[13] G. F. Chen, Z. Li, J. Dong, G. Li, W. Z. Hu, X. D. Zhang, X. H. Song, P. Zheng, N. L. Wang, and J. L. Luo, Phys. Rev. B **78**, 224512 (2008).
[14] G. Wu, H. Chen, T. Wu, Y. L. Xie, Y. J. Yan, R. H. Liu, X. F. Wang, J. J. Ying, and X. H. Chen, J. Phys.: Condens. Matter **20**, 422201 (2008).
[15] S. Ishida, M. Nakajima, K. Miyazawa, H. Kito, Y. Tomioka, T. Ito, A. Iyo, H. Eisaki, and S. Uchida, Proceedings of the 21st International Symposium on Superconductivity (ISS 2008), Tsukuba, 2008, edited by K. Takita and Y. Yamada (Elsevier B. V., Amsterdam), Physica C (to be published).
[16] T. Terashima, M. Kimata, H. Satsukawa, A. Harada, K. Hazama, M. Imai, S. Uji, H. Kito, A. Iyo, H. Eisaki, and H. Harima, J. Phys. Soc. Jpn. **78**, 033706 (2009).
[17] J.-P. Jan, N. L. Martin, and A. Wenger, Phys. Rev. B **9**, 1377 (1974).
[18] J. A. Osborn, Phys. Rev. **67**, 351 (1945).
[19] H. Kiessig, U. Essmann and W. Wiethaup, Phys. Lett. **71**A, 467 (1979).
[20] N. R. Werthamer, E. Helfand, and P. C. Hohenberg, Phys. Rev. **147**, 295 (1966).
[21] I. B. Shameem Banu, M. Rajagopalan, M. Yousuf, and P. Shenbagaraman, J. Alloys Compd. **288**, 88 (1999).